https://africanjournalofbiomedicalresearch.com/index.php/AJBR
Afr. J. Biomed. Res. Vol. 28(2s) (February 2025); 103 - 110
Research Article

The Embryonic Fibroblast Cells Showed Good Growth And Proliferation On Nanocomposite Hydrogel Scaffolds Based On Chitosan/Sodium Alginate/Halloysite Nanotubes

Hussein Jumaah Hussein[1], Ahmad Poursattar Marjani[2*], and Behzad Zeynizadeh[3*]

[1,2*,3*]Department of Organic Chemistry, Faculty of Chemistry, Urmia University, Urmia, Iran.

***Corresponding Authors:** Ahmad Poursattar Marjani and Behzad Zeynizadeh
*[2]Email: a.poursattar@urmia.ac.ir, [3]Email: bzeynizadeh@gmail.com

Abstract
Biomaterial wound dressings, including hydrogels, engage with host cells to modulate the process of tissue repair. This study aimed to investigate the cell growth and proliferation on hybrid hydrogel beads as biocompatible scaffolds using chitosan (CS) and sodium alginate (Alg), incorporating varying concentrations of halloysite nanotubes (Hal)(CS/Alg/Hal). The already synthesized CS/Alg/Hal was previously characterized using various analytical techniques, including FTIR, XRD, SEM/EDX, and TEM. MEF cells, the mouse embryonic fibroblast cell line, were cultured on different CS/Alg/Hal for 24 or 48 h. The in vitro blood coagulation tests were used to assay the biocompatibility of CS/Alg/Hal. MTT and DAPI-staining assays were used to evaluate cell viability. The expression of genes involved in cell growth and proliferation, PI3K/Akt/mTOR/c-Myc signaling were calculated using real PCR, while protein levels of genes involved in cell stemness (Oct-4 and Sox-2) were measured by ELISA. Data showed the good hemostatic properties of the CS/Alg/Hal. MTT and DAPI-staining assays showed high cell viability and growth in hydrogels, especially for M3 hydrogel. The expression of genes involved in cell growth and proliferation, PI3K/Akt/mTOR/c-Myc signaling, and Oct-4 and Sox-2 proteins were up-regulated in hydrogels, especially in the M3 group ($p<0.05$). This cell signaling supports cell hemostasis and proliferation. Therefore, hydrogels showed hopeful application properties in cell growth and wound healing.

Keywords: Cell proliferation, Chitosan, Halloysite, Hybrid scaffolds, Sodium alginate

***Author of Correspondenece: email:** *a.poursattar@urmia.ac.ir; bzeynizadeh@gmail.com*

Received:02/01/2025 *Accepted: 01/02/2025*

DOI: https://doi.org/10.53555/AJBR.v28i2S.6750

Introduction

Tissue engineering is a science that aims to create biological substitutes that can restore, maintain, and improve the function of damaged tissue [1]. In tissue engineering, a biodegradable material that self-destructs in the body's environment is transformed into a structure similar to one of the damaged tissues or organs. This structure is called a scaffold. Hydrogels consist of biomolecules derived from both synthetic and natural polymers. Their unique quasi-three-dimensional architecture imparts distinctive characteristics [2, 3]. They exhibit a high degree of hydrophilicity, coupled with an impressive swelling capacity, exceptional water retention, biodegradability, biocompatibility, and robust mechanical strength. These attributes render them highly applicable in

various tissue engineering endeavors. Consequently, these scaffolds have gained prominence as valuable constructs within tissue engineering and regenerative medicine. Beyond academic research, scaffolds have made their way into clinical applications and are anticipated to significantly contribute to the repair of numerous tissues [4, 5]. In recent years, research in tissue engineering has increasingly concentrated on developing structures that improve the reparative capabilities associated with wound healing and regeneration [5, 6]. The primary aim is to design scaffolds that successfully direct cellular activity to repair injured skin. Cells necessitate a conducive framework for residence and proliferation and rely on signals to orient themselves towards the most favourable conditions for regeneration [5, 6].

The skin's primary structure comprises two layers: the epidermis, which is the outermost layer, and the dermis, which lies beneath it. The epidermis is a thin, protective barrier composed of cells rich in keratinocytes [7]. In contrast, the dermis is a thicker layer that contains fibroblast cells and a network of collagen, which is crucial in providing the skin with flexibility and strength. Biomaterials used in skin tissue engineering should replicate this bilayer structure. Various materials, including collagen sponges, silicone-chitosan (CS) films, chitosan-gelatin composites, gelatin/chondroitin sulfate, and hyaluronic acid, are employed to create bilayer structures for skin tissue engineering applications [8]. CS and algeniate (Alg) are recognized as particularly advantageous polymers for skin tissue engineering and the regeneration of damaged organs due to their biological properties and biodegradability in vivo. While CS/Alg combinations have demonstrated promising in vitro properties for skin tissue, their effectiveness in vivo has not shown satisfactory results [9]. Research indicates that incorporating a membrane in the upper layer can help mitigate the stress experienced by hydrogels in scaffolds during in vivo studies [7, 10]. A study has shown that wounds treated with CS/agarose hydrogel maintained adequate moisture and hydration levels, effectively preventing dehydration of the injury site and promoting significant cell proliferation within the wound area. This environment facilitated the efficient exchange of essential materials such as nutrients, oxygen, and waste products, while the hydrogel's antibacterial properties were validated by the absence of infection in the affected tissue [11]. Fibroblasts are widely used to regenerate and treat various skin disorders [12]. In this study , we used MEF cells, the mouse embryonic fibroblast cell line, to investigate the biocompatibility of CS/Alg/Hal in vitro.

Materials and Methods

Materials

Phosphate buffer solution (PBS) was purchased from Sigma Aldrich (St. Louis, MO, United States). Methyl Thiazolyl diphenyl Tetrazolium bromide (MTT, Sigma-Aldrich), DAPI (Sigma-Aldrich), DMEM (Gibco), Fetal Bovine Serum (FBS, Gibco), penicillin-streptomycin (Pen-Strep, Gibco), Dimethyl Sulfoxide (DMSO, Sigma-Aldrich) RNA extraction kit (cat. NO: FARBK001; Favorgen), RT² SYBR Green qPCR Mastermix (2) (Cat. No. / ID: 330500), cDNA synthesis kit protocol (Cat. No. / ID: 205311), Oct-4 ELISA Kit (ab235653), Sox-2 ELISA (ab245707). All other chemicals used in the study were of analytical grade and were employed without additional purification.

Instruments

Gene expression was performed using RT-PCR Corbett Rotor Gene 3000 (Qiagen, the Netherland). Absorbance was measured using HF4500 ELISA reader system (Meizheng biotechnology Co, China). An Olympus BX50 fluorescence microscope (Olympus Corporation, Japan) was also used to monitor DAPI staining.

The in vitro blood coagulation test

The entire blood coagulation time was assessed. A hydrogel (1 mg) was mixed with 1 mL of blood and incubated at 37 °C for 5 minutes. Then, 50 µL of $CaCl_2$ (0.2 M) was added to initiate coagulation. The blood sample was then agitated in a 37 °C water bath until complete coagulation occurred, at which point the coagulation time was recorded. The blood coagulation index (BCI) was employed to evaluate the coagulation capacity of the material. The hydrogel and 25 µL of whole blood were incubated at 37 °C for 5 minutes. Following this, 2.5 µL of $CaCl_2$ (0.2 M) was gradually introduced into the blood sample, and the EP tube was gently agitated to mix the $CaCl_2$ solution with the blood thoroughly. The EP tube was then incubated in a 37 °C water bath for 1, 2, 3, 4, and 5 minutes. Afterwards, the EP tube was removed from the water bath, and 3 mL of deionized water was carefully added to release the uncoagulated blood without disrupting the formed clot. Finally, the supernatant was aspirated, and the absorbance was measured at 540 nm. The absorbance of untreated 25 µL of whole blood subjected to recalcification for the corresponding time served as a negative control. The coagulation properties of the hydrogels were assessed using the following equation.

$$\mathrm{BCI}\ (\%) = (\mathrm{As} - \mathrm{Aw}) \div (\mathrm{An} - \mathrm{Aw}) \times 100$$

Where As, Aw, and An represents the absorbance values of deionized samples., water, and control groups with negative results, respectively.

Cell culture

MEF cells, the mouse embryonic fibroblast cell line, were obtained from the cell bank unit of the experimental therapy department at the Iraqi Center for Cancer and Medical Genetic Research (ICCMGR) and cultured with DMEM containing 10% FBS (v/v), 1% of streptomycin (v/v) and kept in a humidified incubator (37 °C and 5% CO_2). Cells were incubated in a normal growth medium until they reached 80% confluence. The supernatant was replaced each 2–3 days with fresh medium. For subculture, cells were detached by adding 0.25% trypsin and allocated into proper cell

culture plates for downstream experiments. Cells in passages 5–7 were used for the experiment in triplicate.

Cell viability experiment

To assess cytotoxicity, 0.5 mg hydrogels were sterilized with 70% ethanol. Next, they were rinsed with PBS three times and placed on 96-well tissue cell culture plates. Next, 7 $\times 10^3$ MEF were seeded on the hydrogels in DMEM containing 10% FBS, and 1% pen-strep and kept in a humidified incubator, triplicate for each group. After 24, 48, and 72 h, the cell medium was removed, and MTT solution (5 mg/mL) was added to each well for 4 hours in an incubator. Next, the MTT solution was removed, and DMSO (100 µl) was added to each well for 20 min. To end, the absorbance of each well was measured by an ELISA reader at 570 nm to calculate cell viability according to the formula: Cell viability (%) = absorbance of sample/ absorbance of control ×100.

DAPI staining

DAPI staining was used to stain the nuclei of living MEF cells. In brief, hydrogels were located in 12-well plates and decontaminated with 70% ethanol. After washing with PBS, cells were incubated with the hydrogels, and after 48 h, the supernatant was removed. Next, each well was washed with PBS and fixed with 4% formaldehyde at room temperature (RT) for 15 min. Then, the MSCs were washed three times with PBS, and a DAPI staining solution (0.1%) was added to each well, and the solution was incubated at RT in the dark. After 10 min, the DAPI solution was removed and washed with PBS. An Olympus BX50 fluorescence microscope at × 10 magnification field observed and imaged stored cells.

RNA isolation

MEF cells were incubated in the hydrogels for three days. We used an RNA extraction kit to isolate total RNA from the experimental groups. Initially, 350 µl of FARP and 3.5 µl of β-mercaptoethanol were added to the cells and incubated for 5 minutes. Subsequently, the samples were transferred to a filter column and centrifuged at 18,000 g for 2 minutes at 4 °C. The resulting supernatant was combined with an equal volume of 70% ethanol and then moved to a new filter column. After another centrifugation at 18,000 g for 2 minutes at 4 °C, wash buffers 1 and 2 were applied to the filter column, followed by an additional centrifugation for 1 minute at 4 °C. The filter columns underwent centrifugation for 3 minutes to eliminate any residual liquid. Finally, 100 µl of H_2O was added, and the samples were centrifuged for 1 minute at 4 °C. The purity and concentration of the extracted RNAs were assessed using a nanodrop system (EPOCH/BioTek).

cDNA and Real-time PCR

For the cDNA synthesis, 800 ng of RNA was used to make cDNA according to the cDNA synthesis kit protocol. Real-time PCR was used for measuring gene expression of PI3K, Akt, mTOR, c-Myc, and IL-1β using the primers presented in Table 1, cDNA samples were used to examine the expression of genes using RT² SYBR Green qPCR Mastermix and a MIC Real-Time PCR System (Swiss). The real-time PCR program was: 94 °C for 5 s, 94 °C for 10 s, 58/61°C for 25 s, and 72 °C for 20 s set on 40 cycles. β-Actin was used as a housekeeping gene for normalization. Method 2 (−ΔΔCT) was used to investigate relative changes in gene expression level.

Table 1. Primer sequences.

Gene	Sequences	Tm
PI3K	Forward ACACCACGGTTTGGACTATGG Reverse GGCTACAGTAGTGGGCTTGG	61
Akt	Forward ATAATATGGAACCTTCCCTCCAA Reverse GTCTGTCTCATTCACTGCCCTAC	61
mTOR	Forward ATGTACCCCAACGATGTAACCA Reverse CGGCGTAATGTCCAGACCCA	61
c-Myc	Forward CCA GTA GCG ACT CTG AGG AAG Reverse TGT GAG GAG GTT TGC TGT GG	61
IL-1β	Forward CCACAGACCTTCCAGGAGAATG Reverse GTGCAGTTCAGTGATCGTACAGG	61
B-actin	Forward TGACAGGATGCAGAAGGAGA Reverse TAGAGCCACCAATCCACACA	58

The enzyme-linked immunosorbent assay (ELISA)

To quantify the Oct-4 and Sox-2 proteins, MEF cells were lysed as previously described. Then, the assays were conducted using an Oct-4 ELISA Kit and Sox-2 ELISA kits, following the manufacturer's instructions. In summary, after adding standards, 50 µl of each sample was placed in a plate and incubated for 60 minutes on a shaker at RT. The plates were then washed three times with 250 µl of washing solution. Following this, 50 µl of the conjugated antibody was added to each sample and incubated for 60 minutes on a shaker at RT. The plates were washed thrice, after which 50 µl of HRP-Avidin solution was added to each sample and shaken for 30 minutes. The plates underwent five washes before 50 µl of substrate was mixed with the samples and incubated for 15 minutes. Finally, 25 µl of stop solution was added to each sample, and the absorbance was measured using an ELISA reader at a wavelength of 450 nm.

Statistical analysis

GraphPad Prism 10 was used to analyze the data. One-way ANOVA was used for multiple comparison tests. All the experiments were repeated no less than three times. The data shown represent mean ± SD. $P < 0.05$ was considered statistically significant.

Results and discussion

The in vitro blood coagulation test

BCI quantifies a sample's capacity to promote thrombosis, reflecting its sensitivity to hemolysis. In brief, a lower BCI indicates enhanced coagulation potential of the material. The procoagulant properties of the hydrogel were evaluated by measuring the BCI at intervals of 1 to 5 minutes. As illustrated in Figure 1, all dressing groups containing Hal exhibited a markedly improved procoagulant effect. Notably, the BCI values for M9 and M3 experienced a significant decline after 3 and 4 minutes, respectively. However, with a further increase in Hal concentration, the reduction in BCI became less pronounced, as observed in the M6 and M9 hydrogels. In conclusion, M3 demonstrated the most favourable procoagulant capacity. These findings indicate that the M3 hydrogel possesses excellent biocompatibility and clotting characteristics, making it suitable for managing wound bleeding.

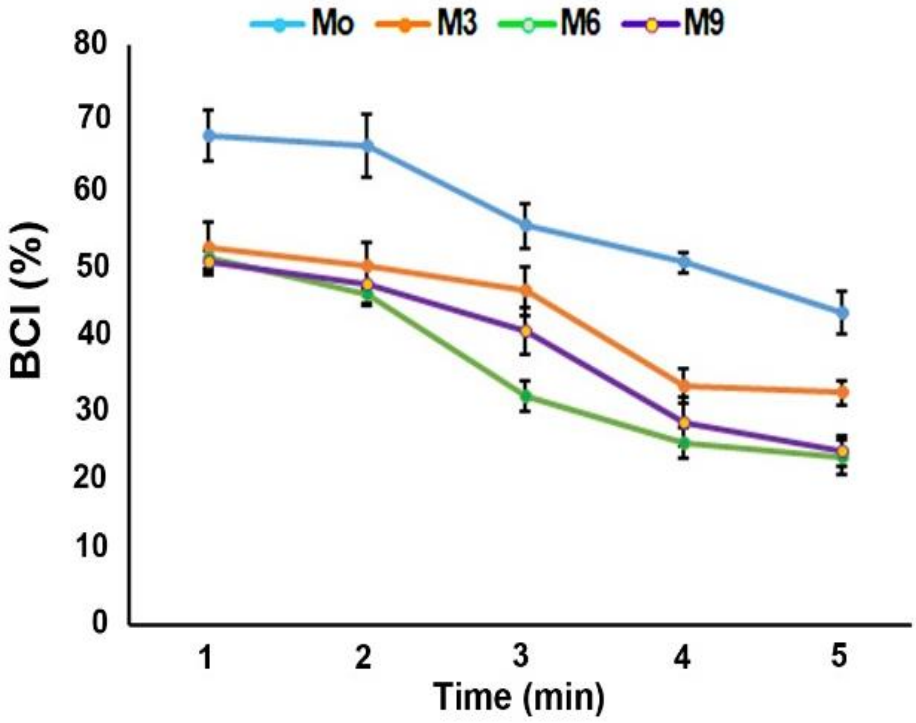

Figure 1. The in vitro blood coagulation test.

Cell viability

Cell viability test showed that nanocomposite hydrogel slightly decreased the viability values of cells after 24 h. However, there was a significant difference between the control group and the M9 group ($p<0.05$) (Figure 2A). After 48 h of incubation, the cell viability of cells in the M6 and M9 groups was significantly decreased ($p<0.05$). At 72 h after treatment, compared to the control group, the cell viability of M0, M6, and M9 was decreased significantly ($p<0.05$). We found that the cell viability of the M3 group was slightly reduced after 24, 48, and 72 h of incubation. In addition, we found that the cell viability value of M3 was high after 24 h (95.26 ±1.51 %), 48 h (93.2 ± 1.7 %) and 72 h (94.53 % ± 3 %) compared to other groups (Fig. 2A). The maximum value of cell viability was 95.53 % ± 3 % for M3 and the minimum one was 79.62 % ± 4.05% for M9 after 72 h (Fig. 2B).. These data showed that the M3 group was more biocompatible to MEF cells. Cell viability is a frequently assessed product characteristic for therapeutic devices incorporating cells [13]. A study demonstrated that aminated-chitosan/alginate/Hal composite scaffolds showed excessive possibility for use in tissue engineering, perfectly in cell culture systems because the cell viability was high and cells had better growth on them [14]. Overall, MEF cells could grow on hydrogels (mainly in the M3 group), suggesting biocompatibility of hydrogels, which is vital for cell hemostasis and growth in the wound healing process [15].

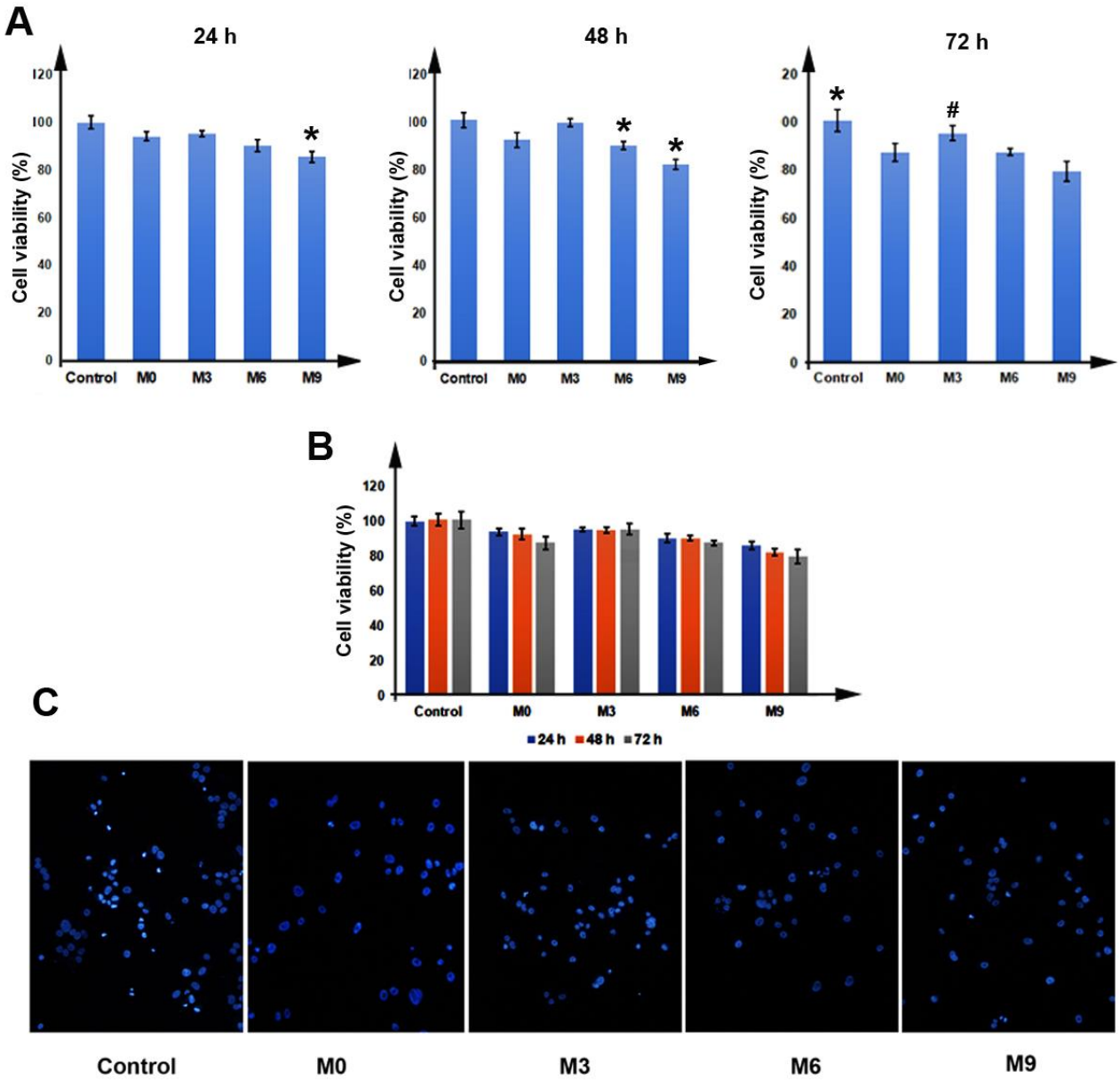

Figure 2. Cell viability for nanocomposite hydrogel was performed by simple MTT assay at 24, 48, and 72 h of incubation. *n* = 3 independent samples; One-way ANOVA followed by Tukey's HSD post hoc test). * means P<0.05, # means P>0.05.

DAPI staining

DAPI staining was used to measure MEF cells' cell viability and growth incubated with different hydrogels after 48 h. As shown in Figure 2C, the DAPI staining images exhibited that 48 h after incubation, cells were visible in cell culture wells, and when compared to the control cells, the number of nuclei was normal. These results indicated that MEF cells could grow and proliferate on hydrogels, confirming the biocompatibility of hydrogels [16].

Real-time PCR

The expression of genes involved in cell growth and proliferation including PI3K, Akt, mTOR, c-Myc, and gene IL-1β involved in inflammation was measured by Real-time PCR (Figure 3A). Results showed that the expression level of the PI3K gene was increased in nanocomposite hydrogels but was significantly high in the M3 group (1.86 ± 0.15 fold change) compared to other groups (p<0.05)(Figure 3A). The same results were obtained for Akt (1.88 ± 0.17 fold change), mTOR (1.83 ± 0.23 fold change), and c-Myc (1.88 ± 0.28 fold change) genes when compared to other groups (p<0.05). In addition, we found that the expression level of IL-1β was down-regulated only in the M3 group (0.71 ± 0.28 fold change) compared to other groups (p<0.05). In contrast, compared to the control group, the expression level of IL-1β was slightly increased in M0 (1.28 ± 0.18 fold change), M6 (1.73 ± 0.17 fold change), and M9 (1.47 ± 0.19 fold change) groups (p>0.05). There was a significant difference between M3 and M9 groups (p<0.05). The

PI3K/Akt/mTOR/c-Myc pathway participates in the signal transduction network in eukaryotic cells, which promotes cell survival, growth, and proliferation [17]. The PI3K/Akt signaling pathway directly impacts mTOR, particularly mTORC1. Akt can enhance the activity of mTORC1, which results in elevated protein synthesis and cellular growth [18]. C-Myc is an oncogene signaling pathway regulating different biological processes including proliferation, differentiation, apoptotic cell death, and cell survival [19]. Findings from this analysis confirm the results of the MTT assay DAPI-staining test. In our study, it seems that an increase in the expression of this axis is associated with cell growth and maintenance on hydrogels. We also found that the expression of IL-1β was low in the M3 group, indicating an inhibition in the inflammatory response of MEF cells cultured on hydrogel [20]. IL-1β was high in M9 hydrogels, possibly due to the high level of Hal causing inflammation response of MEF cells. IL-1β is a potent pro-inflammatory cytokine secreted by innate immune system cells [21]. There is evidence that fibroblasts and other stem cells such as mesenchymal stem cells, also produce different cytokines like IL-1β [22, 23]. Therefore, M3 did not stimulate MEF cells to produce IL-1β, suggesting more biocompatibility of this hydrogel.

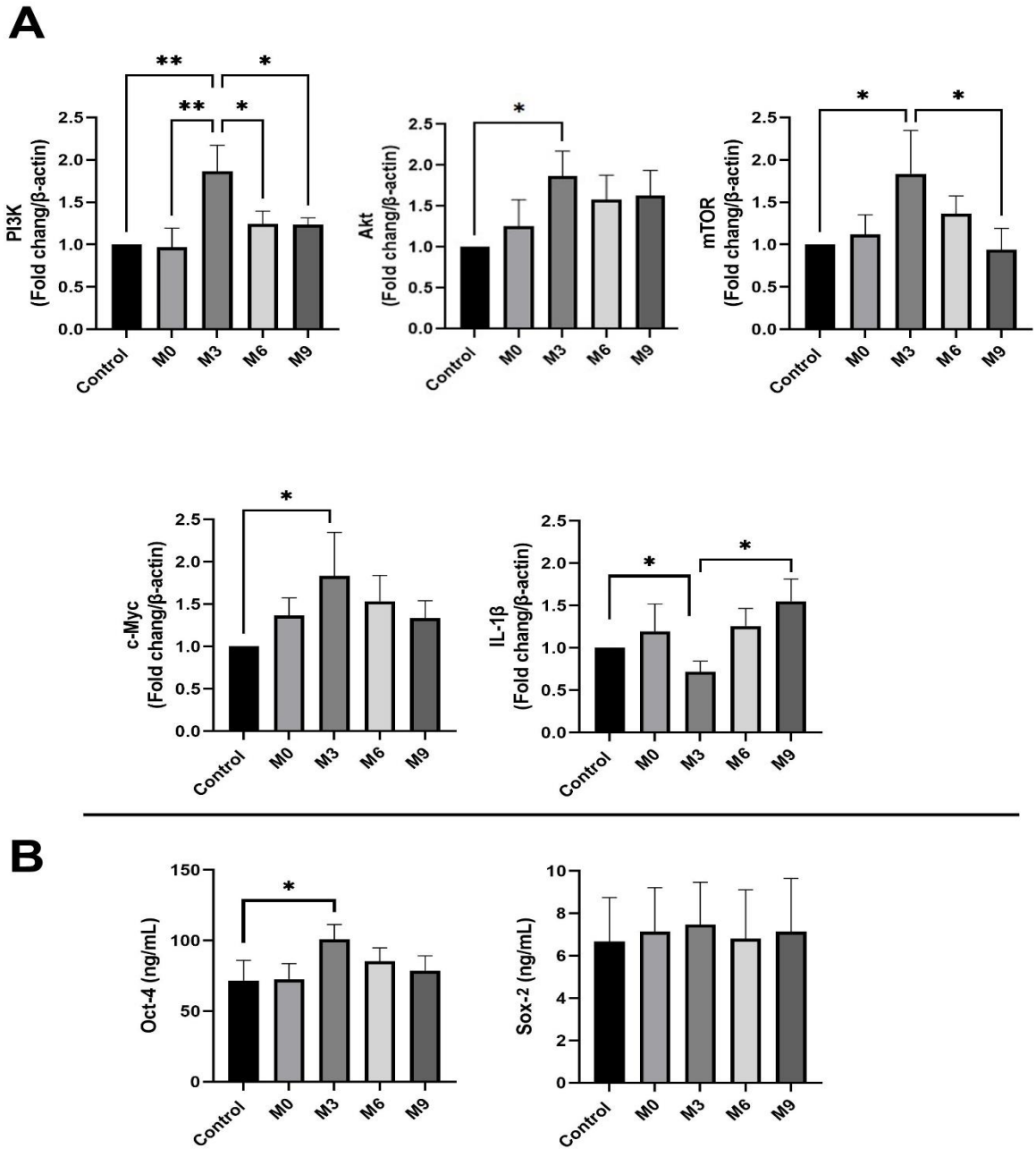

Figure 3. Real-time PCR assay for cell growth and proliferation genes including PI3K, Akt, mTOR, c-Myc, and gene IL-1β involved in inflammation (A). ELISA for proteins OCT-4 and Sox-2 (B). *n* = 3 independent samples; One-way ANOVA followed by Tukey's HSD post hoc test). * means P<0.05.

ELISA

To investigate proteins involved in cell stemness and growth, ELISA was performed for Oct-4 and Sox-2. As shown in Fig. 3B, the protein level of Oct-4 was high in cells incubated with nanocomposite hydrogels; however, it was significantly high in the M3 group (100.8 ± 9.2 ng/ml) compared to the control group (71.67 ± 8.2 ng/mL) ($p<0.05$). No significant changes were found in the protein levels of Sox-2 in all groups ($p>0.05$). Different factors regulate the pluripotency and stemness of stem cells. Oct-4, a POU transcription factor family member, is essential to the machinery that leads to pluripotency [24]. Oct-4 triggers regulation of both protein-coding genes and noncoding RNAs crucial to pluripotency [25]. Therefore, an increase in Oct-4 expression may correlate with the biocompatibility of hydrogels that allow MEF cells to continue stemness and proliferation. Sox-2 is a vital developing transcription factor that mediates stemness, progenitor growth, and multiple growing pathways [26]. SOX-2 has been implicated in the maintenance and differentiation of adult stem cells. It seems that elevated levels of both Oct-4 and Sox-2 regulate MEF cell growth and hemostasis in hydrogels, especially in M3 hydrogel [27].

Conclusion

In summary, hydrogels showed good hemostatic properties. Cell viability and growth were good in hydrogels, especially in the M3 group. The expression of genes in PI3K/Akt/mTOR/c-Myc signaling and Oct-4 and Sox-2 proteins were high, especially in the M3 group. This cell signaling supports cell hemostasis and proliferation. Therefore, these hydrogels showed hopeful application properties in cell growth and supporting wound healing.

Acknowledgments

The authors would like to acknowledge the support from the Research Council of Urmia University.

References

[1] Ikada Y: Tissue engineering: fundamentals and applications: Elsevier; 2011.

[2] Clegg JR, Adebowale K, Zhao Z, Mitragotri S: Hydrogels in the clinic: An update. Bioengineering & Translational Medicine 2024, 9(6):e10680.

[3] Yang D: Recent advances in hydrogels. Chemistry of Materials 2022, 34:1987-1989.

[4] Eming SA, Martin P, Tomic-Canic MJStm: Wound repair and regeneration: mechanisms, signaling, and translation. Science Translational Medicine 2014, 6(265):265sr6.

[5] Chen D, Hou Q, Zhong L, Zhao Y, Li M, Fu XJSCI: Bioactive molecules for skin repair and regeneration: progress and perspectives. Stem Cells International 2019:6789823.

[6] Amor IB, Emran TB, Hemmami H, Zeghoud S, Laouini SEJIJoS: Nanomaterials based on chitosan for skin regeneration: an update. International Journal of Surgery 2023, 109(3):594-596.

[7] Ng WL, Yeong WY, Naing MWJIJB: Polyelectrolyte gelatin-chitosan hydrogel optimized for 3D bioprinting in skin tissue engineering. International Journal of Bioprinting 2016, 2(1):53-62.

[8] Franco RA, Min Y-K, Yang H-M, Lee B-TJJoba: Fabrication and biocompatibility of novel bilayer scaffold for skin tissue engineering applications. Journal of Biomaterials Applications 2013, 27(5):605-615.

[9] Kibungu C, Kondiah PP, Kumar P, Choonara YEJFiM: This review recent advances in chitosan and alginate-based hydrogels for wound healing application. Frontiers in Materials 2021, 8:681960.

[10] Arabpour Z, Abedi F, Salehi M, Baharnoori SM, Soleimani M, Djalilian ARJIJoMS: Hydrogel-Based Skin Regeneration. International Journal of Molecular Sciences 2024, 25(4):1982.

[11] Miguel SP, Ribeiro MP, Brancal H, Coutinho P, Correia IJJCp: Thermoresponsive chitosan–agarose hydrogel for skin regeneration. Carbohydrate Polymers 2014, 111:366-373.

[12] Hyun J, Eom J, Im J, Kim Y-J, Seo I, Kim S-W, Im G-B, Kim YH, Lee D-H, Park HS et al: Fibroblast function recovery through rejuvenation effect of nanovesicles extracted from human adipose-derived stem cells irradiated with red light. Journal of Controlled Release 2024, 368:453-465.

[13] Babakhanova G, Agrawal A, Arora D, Horenberg A, Budhathoki JB, Dunkers JP, Chalfoun J, Bajcsy P, Simon Jr CG: Three-dimensional, label-free cell viability measurements in tissue engineering scaffolds using optical coherence tomography. Journal of Biomedical Materials Research Part A 2023, 111(8):1279-1291.

[14] Amir Afshar H, Ghaee A: Preparation of aminated chitosan/alginate scaffold containing halloysite nanotubes with improved cell attachment. Carbohydrate Polymers 2016, 151:1120-1131.

[15] Fernández-Guarino M, Hernández-Bule ML, Bacci SJB: Cellular and molecular processes in wound healing. Biomedicines 2023, 11(9):2526.

[16] Kang R, Luo Y, Zou L, Xie L, Lysdahl H, Jiang X, Chen C, Bolund L, Chen M, Besenbacher FJRA: Osteogenesis of human induced pluripotent stem cells derived mesenchymal stem cells on hydroxyapatite contained nanofibers. RSC Advances 2014, 4(11):5734-5739.

[17] Glaviano A, Foo ASC, Lam HY, Yap KCH, Jacot W, Jones RH, Eng H, Nair MG, Makvandi P, Geoerger B et al: PI3K/AKT/mTOR signaling transduction pathway and targeted therapies in cancer. Molecular Cancer 2023, 22(1):138.

[18] Dibble CC, Cantley LCJTicb: Regulation of mTORC1 by PI3K signaling. Trends in Cell Biology 2015, 25(9):545-555.

[19] Ashrafizadeh M, Zarabi A, Hushmandi K, Moghadam ER, Hashemi F, Daneshi S, Hashemi F, Tavakol S, Mohammadinejad R, Najafi MJCcdt: C-Myc signaling pathway in treatment and prevention of brain tumors. Current Cancer Drug Targets 2021, 21(1):2-20.

[20] Dinarello CA, Simon A, Van Der Meer JWJNrDd: Treating inflammation by blocking interleukin-1 in a broad spectrum of diseases. Nature Reviews Drug Discovery 2012, 11(8):633-652.

[21] Lopez-Castejon G, Brough DJC, reviews gf: Understanding the mechanism of IL-1β secretion. Cytokine & Growth Factor Reviews 2011, 22(4):189-195.

[22] Viveiros MMH, de Melo Viveiros ME, Silva MG, Kaneno R, Avelino NP, Rainho CA, Schellini SAJSCI: Expression of inflammatory cytokines in mesenchymal stem cells derived from proximal humerus fractures. Stem Cell Investigation 2022, 9:3.

[23] Wei K, Nguyen HN, Brenner MBJTJoci: Fibroblast pathology in inflammatory diseases. Journal of Clinical Investigation 2021, 131(20): e149538.

[24] Jerabek S, Merino F, Schöler HR, Cojocaru V: OCT4: Dynamic DNA binding pioneers stem cell pluripotency. Biochimica et Biophysica Acta (BBA) - Gene Regulatory Mechanisms 2014, 1839(3):138-154.

[25] Shi G, Jin Y: Role of Oct4 in maintaining and regaining stem cell pluripotency. Stem Cell Research & Therapy 2010, 1(5):39.

[26] Zhang S, Cui WJWjosc: Sox2, a key factor in the regulation of pluripotency and neural differentiation. World Journal of Stem Cells 2014, 6(3):305-311.

[27] Matic I, Antunovic M, Brkic S, Josipovic P, Mihalic KC, Karlak I, Ivkovic A, Marijanovic IJOaMjoms: Expression of OCT-4 and SOX-2 in bone marrow-derived human mesenchymal stem cells during osteogenic differentiation. Open Access Macedonian Journal of Medical Sciences 2016, 4(1):9-16.